Quantifying the Effects of Non-hydrostatic Stress on Single-component Polymorphs

Benjamin L. Hess[1*] and Jay J. Ague[1,2]

[1] Department of Earth and Planetary Sciences, Yale University, PO Box 208109, New Haven, CT 06520-8109, USA.

[2] Yale Peabody Museum of Natural History, Yale University, New Haven, CT 06511, USA

Corresponding author: Benjamin Hess (Benjamin.hess@yale.edu)

Key points:

1) Normal stress determines chemical potential and consequent phase stability on a given interface to first order.
2) Interface-parallel stresses can influence phase stability for interfaces near a reaction boundary.
3) Non-hydrostatic thermodynamics are directly applicable to dry systems undergoing solid-solid reactions.

ABSTRACT:

Gibbs free energy, the fundamental thermodynamic potential used to calculate equilibrium mineral assemblages in geological systems, does not apply to non-hydrostatically stressed solids. Consequently, there is debate over the significance of non-hydrostatic stress in petrological and geophysical processes. To help resolve this debate, we consider the effects of non-hydrostatic stress on the polymorph pairs kyanite/sillimanite, graphite/diamond, calcite/aragonite, and quartz/coesite. While these polymorphs are most relevant to metamorphic processes, the concepts developed are applicable to any single-component solid reaction. We quantitatively show how stress variations normal to an interface alter equilibrium temperatures of polymorph pairs by approximately two orders of magnitude more than stress variations parallel to an interface. Thus, normal stress controls polymorph stability to first order. High-pressure polymorphs are expected to preferentially nucleate normal to and grow parallel to the maximum stress and low-pressure polymorphs, the minimum stress. Nonetheless, stress variations parallel to an interface allow for the surprising possibility that a high-pressure polymorph can become more stable relative to a low-pressure polymorph as stress decreases. The effects of non-hydrostatic stress on mineral equilibrium are unlikely to be observed in systems with interconnected, fluid-filled porosity, as fluid-mediated reactions yield mineral assemblages at approximately constant pressures. In dry systems, however, reactions can occur directly between elastic solids, facilitating the direct application of non-hydrostatic thermodynamics. Non-hydrostatic stress is likely to be important to the evolution of metamorphic systems, as preferential orientations of polymorphic reactions can generate seismicity and may influence fundamental rock properties such as porosity and seismic anisotropy.

Plain language summary:

Geoscientists are interested in determining at what temperatures and pressures different minerals are stable in the Earth. This is because the breakdown and formation of minerals is important for processes such as the generation of earthquakes and the geochemical cycling of elements like hydrogen and carbon. However, a key problem is that the calculations we use to determine if minerals are stable assume that pressure is equal in all directions. But if this were true, there would be no mountains or earthquakes which are caused by unequal pressures deep within our planet. This leaves the question of how do we determine mineral stability when pressure is not equal in all directions? In our work, we show that the pressure on each side of a mineral determines whether each side is stable. This means, for example, if one squeezes graphite hard enough in one direction, the squeezed sides will start to form diamond while the other sides remain graphite. Consequently, when pressure is not equal in all directions, minerals will break down or form in certain directions. This could create cracks for earthquakes, or allow water to enter rocks more easily, influencing subsurface fluid flow and element cycling.

1. Introduction

Gibbs free energy (G) is the fundamental thermodynamic potential that forms the backbone of analytical techniques used in geology such as pseudosection modeling and geothermobarometry. It was defined by Gibbs (1875) as

$$G = E - TS + PV \qquad (1)$$

where E is internal energy, T is absolute temperature, S is entropy, P is pressure, and V is volume. Gibbs free energy has the special property that when a system's temperature and pressure are constant, the molar G value, or chemical potential, of each component in a system

will be equal in all phases at chemical equilibrium. This foundational thermodynamic principle is used to determine equilibrium stability relationships in chemical systems of any complexity. A basic example is determining the pressure-temperature conditions of equilibrium among polymorphs, such as the aluminosilicate (Al_2SiO_5) polymorphs, in a single-component system.

An important concern, however, when applying Gibbs free energy to geological systems is that elastic solids can sustain unequal, or "non-hydrostatic," stresses at mechanical equilibrium (Connolly, 2009; Dahlen, 1992; Hobbs & Ord, 2016; Powell et al., 2018; Tajčmanová et al., 2014, 2015; Wheeler, 2014, 2018, 2020). Consequently, the special property of *G* no longer applies. This point was demonstrated by Gibbs himself. He considered the case of a single-component parallelepiped solid in contact with fluids at three different pressures, one per set of parallel faces. He showed that the chemical potential at each solid-fluid interface is (p. 353, 1878)

$$A_s + P_f V_s = \mu_s^f \qquad (3)$$

where *A* is the Helmholtz free energy, the *s* and *f* subscripts refer to solid and fluid, respectively, and μ_s^f is the chemical potential of the solid dissolved in the fluid. The Helmholtz free energy (*A*) is $E - TS$ and can be used to define interface equilibrium conditions. Gibbs showed that since A_s and V_S were constant for the solid but P_f varied between the fluids, the chemical potential of the solid dissolved in each of the three fluids would be different. This demonstrates that the *G*-based chemical potential of a component may not be constant in all phases at equilibrium when stress is non-hydrostatic. Furthermore, the fact that the chemical potential is different at each interface of the non-hydrostatically stressed solid suggests that a *G*-based chemical potential cannot be meaningfully defined ***within*** a non-hydrostatically stressed solid (Kamb, 1961; Larché & Cahn, 1985). The chemical potential within a solid can only be

rigorously defined when the chemical potential is the same on all interfaces, that is, when the solid is hydrostatically stressed and therefore behaves thermodynamically as a fluid phase (Larché & Cahn, 1985). Consequently, a single-valued "thermodynamic pressure" for a solid, such as the mean stress, cannot be used to define a single *G*-based chemical potential for a non-hydrostatically stressed solid and, thus, cannot be used to determine equilibrium assemblages (Bruton & Helgeson, 1983; Kamb, 1961; Larché & Cahn, 1985; Powell et al., 2018; Wheeler, 2018). Instead, equation (3) must be used to determine the specific chemical potential and consequent equilibrium condition at each solid-fluid interface.

It has generally been thought that in fluid-saturated systems, the fluid pressure determines the equilibrium mineral assemblages (Bruton & Helgeson, 1983; Dahlen, 1992; Kamb, 1961). This is because P_f will be constant in a fluid-rock system with interconnected porosity, and A_s and V_S are both relatively insensitive to stress changes. Consequently, the conventional wisdom holds that μ_S^f varies only slightly if solids are non-hydrostatically stressed in fluid-bearing systems. However, the effects of non-hydrostatic stress on solid-solid interfaces and on subsequent equilibrium mineral assemblages is a highly debated topic (Connolly, 2009; Hobbs and Ord, 2016; Powell et al., 2018; Tajčmanová et al., 2014, 2015; Wheeler, 2014, 2018).

In this work we investigate the range of effects of non-hydrostatic stress on both solid-solid and solid-fluid interface equilibria and discuss implications for natural geological systems. We focus specifically on a quantitative treatment of stability relations among single-component polymorphs. We use Larché and Cahn's (1985) equation (3.24) for solid-solid interface equilibrium, which stems from the equilibrium conditions defined in equations (25), (26), and (27) in Larché and Cahn (1978b). The work of Larché and Cahn (1973, 1978a, 1978b, 1985) closely follows Gibbs' derivations and extends them to define mechanical, thermal, and chemical

equilibrium in systems with both fluids and non-hydrostatically stressed, multi-component elastic solids which allow diffusion. Larché-Cahn theory has been both well established in the materials science community and experimentally tested (e.g., Shi et al., 2018). Wheeler (2018) presented Larché and Cahn's equation (3.24) simplified for the case of two single-component solids:

$$A^{\alpha} - \sigma_n V^{\alpha} = A^{\beta} - \sigma_n V^{\beta} \qquad (4)$$

where A and V are the molar Helmholtz free energies and volumes, respectively, of two phases α and β, and σ_n is the normal stress between α and β. This equation represents the condition for chemical equilibrium between two single-component polymorphs such as kyanite and sillimanite at a given interface. When the chemical potentials of both phases are equal, they are in chemical equilibrium at that interface. We use the standard sign convention that compressive stress on a solid is negative and tension is positive in accordance with traditional linear elastic theory; in contrast, pressure in a fluid is positive by convention as a fluid cannot support tensile stress (Larché & Cahn, 1985). This means that equation (4) has minus signs in front of terms containing normal stress whereas (3) has a plus sign in front of the fluid pressure term. Additionally, we note that when one of the solids is hydrostatically stressed, equation (4) simplifies to (3) because a hydrostatically stressed solid behaves as a fluid thermodynamically (Gibbs, 1875; Larché & Cahn, 1985). When both solids are hydrostatically stressed, it becomes the classic G equilibrium condition.

Previous studies have illuminated key aspects of polymorphic relationships under non-hydrostatic conditions. For example, Powell et al. (2018) use a solution to equation (4) which is Larché and Cahn's (1985) equation (4.30) simplified for single-component solids using the derivation from Sekerka and Cahn (2004). They use this to investigate the effects of stress

variations parallel to an interface on aluminosilicate polymorph phase relations. They conclude that non-hydrostatic stress has a smaller effect on solid-solid interface equilibrium than it has on solid-fluid interface equilibrium, making non-hydrostatic stress inconsequential in determining equilibrium mineral assemblages. Wheeler (2018, 2020) presents equation (4) but argues that variation in normal stress controls equilibria and qualitatively discusses previously published experiments that support this hypothesis. In contrast to Powell et al. (2018), Wheeler (2014) posits that normal stress variations could locally alter the equilibrium temperature of metamorphic reactions by hundreds of degrees. Thus, there is continued debate over the significance of non-hydrostatic stress on phase relations in geological systems. Resolving this debate has fundamental implications for interpretation of metamorphic phase relations and fluid-rock systems in general.

These previous studies have each highlighted a different piece of how stress affects mineral equilibria. Wheeler (2014) focuses on variation in stresses normal to mineral interfaces during metamorphic reactions while Powell et al. (2018) implicitly consider variations in stresses parallel to mineral interfaces during polymorphic replacement reactions. Consequently, what is required now is a full 3-dimensional quantitative assessment of how stress affects solid-fluid and solid-solid interface equilibrium that can help reconcile previous results and serve as a foundation for further investigations of the effects of non-hydrostatic stress.

Here we quantitatively show how variations in non-hydrostatic stress can shift interface equilibrium temperatures by a few degrees to hundreds of degrees, unifying previous results. We do this by applying a three-dimensional extension of equation (4) to four significant geological single-component polymorphs: kyanite/sillimanite (Al_2SiO_5), quartz/coesite (SiO_2), calcite/aragonite ($CaCO_3$), and graphite/diamond (C). We focus on kyanite and sillimanite to

demonstrate the full range of effects of non-hydrostatic stress on the stability of both solid-fluid and solid-solid interfaces for comparison with Powell et al. (2018; Figure 1). For the other three pairs of polymorphs, results are provided only for the solid-solid case as it is the focus of this paper (Figure 2). We examine direct reactions between a solid phase and another solid or fluid phase. Thus, our calculations do not consider more complex fluid behaviors such as grain boundary films that can sustain non-hydrostatic stresses between mineral grains (e.g., Alcantar et al., 2003; Kristiansen et al., 2011; Rutter, 1983) or reactions involving interface-coupled dissolution-reprecipitation (e.g., Ague & Axler, 2016; Putnis & Austrheim, 2010; Putnis & John, 2010). While the polymorphs we examine are relevant to metamorphic processes, the concepts developed in this work are directly applicable to any single-component solid reaction and, therefore, to a wide range of lithospheric settings.

2. Methods

Here we derive a three-dimensional form of equation (4), showing how A, V, and σ_n can be computed for an arbitrary stress state. For A, first calculate the molar Gibbs free energy of formation for the phase of interest at a hydrostatic pressure and temperature of interest, $\Delta G_{f,T,P}$, and subtract the pressure times the molar volume at the pressure and temperature of interest, $V_{T,P}$, as this is by definition A:

$$\Delta A_{f,T,P} = \Delta G_{f,T,P} - PV_{T,P} \qquad (5)$$

where $\Delta A_{f,T,P}$ is the Helmholtz free energy of formation at the given temperature and pressure. Next, using linear elastic theory with a small strain approximation (e.g., Voorhees & Johnson, 2004, p. 38-41), determine the change in A between the hydrostatic pressure and the stress of

interest at a constant temperature by integrating the following equation (e.g., Nye, 1957, p. 136-137):

$$dA = V_T \sigma_{ij} d\varepsilon_{ij} \qquad (6)$$

where dA is an infinitesimal increment of A, V_T is the volume at the temperature of interest with no stress ($\sigma_{ij} = \mathbf{0}$), σ_{ij} is the Cauchy stress tensor, and $d\varepsilon_{ij}$ is an infinitesimal increment of the small strain tensor ε_{ij}. The ij follow indicial notation and repeated indices (ii) follow the Einstein summation convention. When integrated from a reference hydrostatic pressure, $\sigma_P = -P$ (compressive stress is negative), equation (6) becomes

$$A_\sigma = \Delta A_{f,T,P} + \frac{1}{2} V_T \left[\sigma_{ij}\varepsilon_{ij} - 3\sigma_P \varepsilon_P\right] = \Delta G_{f,T,P} - P V_{T,P} + \frac{1}{2} V_T \left[\sigma_{ij}\varepsilon_{ij} - 3\sigma_P \varepsilon_P\right] \qquad (7)$$

where A_σ is the Helmholtz free energy at the stress σ_{ij}, and ε_P is the axial strain at the reference hydrostatic pressure (P).

Next, the molar volume at the stress of interest, V_σ, can be calculated by taking the sum of one plus the diagonal components of the strain tensor (i.e., the dilation) and multiplying this by the original volume, V_T:

$$V_\sigma = V_T(1 + \varepsilon_{ii}). \qquad (8)$$

This is a valid approximation of the volume if strains are small (<3–4%; Voorhees & Johnson, 2004, p. 42).

Lastly, normal stress can be calculated by multiplying the Cauchy stress tensor by the components of the unit vector normal to the interface, **n** (Larché and Cahn, 1985):

$$\sigma_n = \sigma_{ij} n_i n_j. \qquad (9)$$

Thus, using equations (7), (8), and (9), equation (4) can be rewritten as

$$A_\sigma^\alpha - \sigma_{ij}^\alpha n_i^\alpha n_j^\alpha V_T^\alpha (1 + \varepsilon_{ii}^\alpha) = A_\sigma^\beta - \sigma_{ij}^\beta n_i^\beta n_j^\beta V_T^\beta (1 + \varepsilon_{ii}^\beta) \qquad (10)$$

where α and β are again the two single-component phases of interest such as kyanite and sillimanite. Equation (10) can be solved to determine chemical equilibrium for an interface at any orientation between two single-component solids of arbitrary symmetry in an arbitrary stress field at mechanical and thermal equilibrium (i.e., constant stress and temperature). Note that stresses parallel to the interface need not be equivalent in phases α and β (e.g., Figure 1e). However, they are equivalent in our treatment of solid-solid relationships (Figure 1a) in order to limit the calculations to three independent variables (Figures 1 and 2).

We solve equation (10) to calculate the interface equilibrium temperature at which kyanite and sillimanite are at chemical equilibrium for solid-solid and solid-fluid interfaces depicted in Figures 1a and 1e. We align the principal stresses so they are normal to the faces of the solids. We vary the normal stress between -0.5 and -0.9 GPa and the parallel stresses between -0.1 and -1.3 GPa. For solid-solid interface equilibrium, both the kyanite and the sillimanite are equivalently non-hydrostatically stressed along their axes (Figure 1a). For solid-fluid interface equilibrium, the kyanite is non-hydrostatically stressed while the sillimanite is hydrostatically stressed at a value equal to the normal stress between the kyanite and sillimanite (Figure 1e). The sillimanite in this example is therefore a "fluid" thermodynamically, as hydrostatically stressed solids are treated using fluid (i.e., constant pressure) thermodynamics. However, this does not imply that the sillimanite has the mechanical properties of a fluid.

We also calculate the equilibrium temperature for solid-solid interfaces as depicted in Figure 1a between graphite and diamond (C) with normal stresses from -3.1 to -3.5 GPa and interface-parallel stresses from -2.7 to -3.9 GPa (Figure 2a); calcite and aragonite ($CaCO_3$) with normal stresses from -1.4 to -1.7 and interface-parallel stresses from -1.0 to -2.1 GPa (Figure 2b); and quartz and coesite (SiO_2) with normal stresses ranging from -2.7 to -3.0 GPa and

interface-parallel stresses from -2.3 to -3.4 GPa (Figure 2c). We chose these ranges so that all the polymorph pairs have comparable equilibrium temperatures ranging from approximately 600 to 700 ^{o}C. We emphasize that the computed conditions for equilibrium—when both phases have equivalent chemical potentials—only apply to the specified interface between the two polymorphs (Figures 1a and 1e) and do not imply chemical equilibrium at the other interfaces. We do not consider shear stress because typical geological solid-solid and solid-fluid interfaces cannot sustain shear stress at mechanical equilibrium (Bruton & Helgeson, 1983; Larché & Cahn, 1978b).

The thermodynamic calculations use Holland and Powell's (2011) thermodynamic dataset (HP11). Our elastic calculations treat all polymorphs as isotropic and their elastic moduli as constants. These approximations are valid for assessing the effects of non-hydrostatic stress to first order (Larché & Cahn, 1985; Powell et al., 2018). To determine a full set of isotropic elastic moduli (e.g., Nye, 1957, p. 142-146), we use the bulk moduli from HP11 and a Poisson's ratio of 0.24 for kyanite (Mikowski et al., 2008); 0.27 for sillimanite (Christensen, 1996); 0.084 for quartz (Pabst & Gregorova, 2013); 0.25 for coesite (Chen et al., 2015); 0.31 for calcite and 0.18 for aragonite (Schön, 2011); and 0.223 for graphite and 0.069 for diamond (Gercek, 2007).

3. Results

In the solid-solid interface scenario the same stresses are applied to the three orthogonal axes of each polymorph (Figure 1a). Figures 1b and 2 show equilibrium isothermal surfaces that represent all stress combinations at which the interface is at equilibrium for a given temperature. The greater the change in equilibrium temperature with stress variation, the greater the effect the stress variation has on the phases' chemical potentials and consequent interface equilibrium. For

253 a fixed stress, temperatures higher than the equilibrium temperature will make the high-pressure
254 polymorph (e.g., kyanite) unstable at the interface, and lower temperatures will make the low-
255 pressure polymorph (e.g., sillimanite) unstable.

256 Geometrically, the isothermal surfaces for the Al_2SiO_5, C, and $CaCO_3$ polymorph pairs
257 have a concave-down, inverted "bowl" topology (Figures 1b and 2a-b). The constant normal
258 stress cross sections (e.g., Figure 1c) are elliptical with their centers at the point of hydrostatic
259 stress where normal stress = stress 2 = stress 3. The centers are minima because the equilibrium
260 temperature increases away from them. In contrast, SiO_2 has saddle isothermal surfaces (Figure
261 2c). The constant normal stress cross section has a saddle point for the center where normal
262 stress = stress 2 = stress 3, and equilibrium temperature increases or decreases depending on how
263 stresses 2 and 3 are varied.

264 For the solid-solid Al_2SiO_5 polymorph pair, when the normal stress is varied, the
265 corresponding change in interface equilibrium temperature is large and similar to the kyanite-
266 sillimanite Clapeyron slope: a 0.2 GPa change in normal stress changes the interface equilibrium
267 temperature by ~100 ^oC (Figure 1d). In contrast, if the interface-parallel stresses (stresses 2 and
268 3) are varied by 1 GPa, the interface equilibrium temperature shifts by only a few ^oC (Figure 1c).
269 The other polymorph pairs show similar magnitude variations (Figure 2).

270 In the solid-"fluid" interface scenario (Figures 1e-h), kyanite is non-hydrostatically
271 stressed whereas sillimanite is hydrostatically stressed at a value equal to the normal stress,
272 thermodynamically representing a fluid (Figure 1e; Larché & Cahn, 1985). The isothermal
273 surfaces have a concave-up "bowl" topology (Figure 1f). The constant normal stress cross
274 section has elliptical contours with a center where normal stress = stress 2 = stress 3 (Figure 1g).
275 The center is a maximum because the equilibrium temperature decreases away from it. When

276 the normal stress is varied, the change in the interface equilibrium temperature is large although
277 slightly less than that of the solid-solid scenario: a 0.2 GPa change in normal stress changes the
278 interface equilibrium temperature by ~90 ^{o}C (Figure 1h). In contrast, varying the interface-
279 parallel stresses (stresses 2 and 3) by 1 GPa shifts the interface equilibrium temperature by only
280 ~5 ^{o}C at most (Figure 1g).
281
282 **4. Discussion**
283 Remarkably, the effects of non-hydrostatic stress on interface equilibrium temperature
284 can range over two orders of magnitude, depending on how stress is applied (Figures 1 and 2).
285 The change in equilibrium temperature with stress variation is a physically intuitive way of
286 understanding the influence stress has on the chemical potential of the given interface.
287 **4.1. Normal stress controls interface equilibrium conditions**
288 The results demonstrate that normal stress determines the equilibrium temperature of an
289 interface to first order (Bruton and Helgeson, 1983; Ferry, 2000; Gibbs, 1878; Green, 1980;
290 Karato, 2008; Larché & Cahn, 1985; Paterson, 1973; Richter et al., 2016; Robin, 1978; Vaughan
291 et al., 1984, Wheeler, 2014, 2018, 2020). This intuitively makes sense as the normal stress is the
292 stress that some chemical species on the surface of a phase (i.e., an interface) has to overcome to
293 be removed from the current phase and form a new one (Karato, 2008).
294 In contrast, variations in the interface-parallel stresses have only a small effect on
295 equilibrium temperature (Figures 1c, 1g, and 2). The effects of variations in the interface-parallel
296 stresses are what Powell et al. (2018) calculated in their work. The reason interface-parallel
297 stresses have only a small effect on interface equilibrium temperature is that when normal stress
298 is constant, only A_σ and V_σ vary in equation (10). These are functions of elastic strain which

changes only slightly with stress, and therefore, the equilibrium temperature changes only slightly. The variation in the solid-solid case (Figure 1c) is smaller than that of the solid-fluid case (Figure 1g). In the solid-fluid case, A_σ and V_σ change only for kyanite. In the solid-solid case, however, A_σ and V_σ will increase or decrease together for both phases as they are equally non-hydrostatically stressed. This means that in the solid-fluid case, the change in equilibrium temperature corresponds to the change in A_σ and V_σ for kyanite (Figure 1g) whereas in the solid-solid case, the change in equilibrium temperature corresponds to the *difference* in the change of A_σ and V_σ between kyanite and sillimanite (Figure 1c). Consequently, interface-parallel stress variations have surprisingly little effect on the interface equilibrium temperature of polymorphs, consistent with Powell et al. (2018).

However, although the variations of stresses 2 and 3 in Figure 1a may have only a small effect on the interface between kyanite and sillimanite (Figure 1c), they would have large effects on the equilibrium temperatures for interfaces that are normal to them. This indicates that while the interfaces between kyanite and sillimanite examined in Figures 1a and 1e may be at chemical equilibrium at a given temperature and stress, the other interfaces are unlikely to also be at equilibrium. Consequently, for a non-hydrostatically stressed solid, the equilibrium condition of each interface must be determined individually using equation (10). Smaller stress variations of up to 0.1–0.2 GPa, which are common in some metamorphic systems (e.g., Andersen et al., 2008; Devaux et al., 2000; Little et al., 2007; Wheeler, 2014; Zulauf, 2001), would shift interface equilibrium temperatures by as much as 50–100 ^{o}C (Figures 1b and 1d) on interfaces of the same mineral grain depending on its orientation. This suggests that non-hydrostatic stress can have a considerable impact on mineral stability.

The influence of normal stress on interfaces predicts three major effects on polymorphic phase transitions, each of which have been demonstrated experimentally. 1) At a fixed temperature, high-pressure polymorphs should form when the maximum stress exceeds the hydrostatic pressure of transformation, and for low-pressure polymorphs, when the minimum stress falls below the hydrostatic pressure of transformation (Hirth & Tullis, 1994; Richter et al., 2016; Zhou et al., 2005; Figure 3b). 2) High-pressure polymorphs should preferentially nucleate along interfaces normal to the maximum stress while low-pressure polymorphs should preferentially nucleate along interfaces normal to the minimum stress (Cionoiu et al., 2019; Green & Burnley, 1989; Hacker & Kirby, 1993; Kirby et al., 1991; Schubnel et al., 2013; Vaughan et al., 1984; Figure 3c). 3) High-pressure polymorphs may then preferentially grow parallel to the maximum stress, and low-pressure polymorphs, the minimum stress (Hacker & Kirby, 1993; Vaughan et al., 1984).

The first and second effects have recently been demonstrated by Richter et al. (2016). In their quartz/coesite phase transition experiments, coesite, the high-pressure polymorph, formed when the maximum stress exceeded the pressure of the phase transition (Figure 3b). Coesite formation occurred even when the mean stress of the system resided significantly below the quartz/coesite transition pressure (Figure 3a). This provides a clear experimental demonstration that the normal stress on each interface determines phase stability to first order (Figure 3b). In addition, our rose diagram representing the orientation of the coesite grains in Figure 3c strongly suggests that the coesite grains nucleated along interfaces normal to the maximum stress, consistent with the second effect. Subsequent shear strain in these experiments rotated the coesite grains into the shear and foliation planes (Richter et al., 2016; Figure 3c), preventing the third effect (growth parallel to the maximum stress) from being clearly observed as the experiments

progressed. However, growth parallel to the maximum stress has been observed in some previous non-hydrostatically stressed polymorph reaction experiments with lower shear strains (e.g., Hacker & Kirby, 1993; Vaughan et al., 1984).

4.2. Interface stability with interface-parallel stress variation

Although interface-parallel stress variations only shift interface equilibrium temperatures by a small amount, they are still important as they cause phase instabilities at interfaces which are at or near a reaction boundary. How these interface-parallel stresses affect phase stabilities depends on the morphology of the isothermal surfaces (Figures 1b, 1f, and 2).

4.2.1. Solid-fluid case

The solid-fluid case has a concave-up isothermal surface topology (Figure 1f). Consider a kyanite–sillimanite interface that is hydrostatically stressed at a fixed temperature and is at equilibrium. In this case, if either of the kyanite interface-parallel stresses (stresses 2 and 3 in Figure 1e) are increased or decreased, the equilibrium temperature of that interface will decrease (Figure 1g). Consequently, the system temperature now exceeds the equilibrium temperature of the interface, making sillimanite, the low-pressure polymorph, stable relative to kyanite, the high-pressure polymorph. That is, if two polymorphs are hydrostatically stressed and at equilibrium on an interface, any variation in interface-parallel stress on the high-pressure polymorph will make it unstable relative to the low-pressure polymorph. Surprisingly, this means that an *increase* in interface-parallel stress will actually make a high-pressure polymorph *less* stable relative to a hydrostatically stressed low-pressure polymorph.

This result is consistent with and extends the derivation of Sekerka and Cahn (2004). They showed that if 1) a hydrostatically stressed solid is in equilibrium with its melt, and 2) the solid stress is varied parallel to the solid-melt interface, then 3) the solid's melting temperature

will decrease along that same interface. Stated another way, interface-parallel stress variation decreases the melting point of the solid along the given interface. In our case, sillimanite can be viewed as a higher temperature "melt" phase because it remains hydrostatically stressed like a fluid. Additionally, the values of the contours in Figure 1g are consistent with the magnitudes calculated by Sekerka and Cahn (2004). However, we emphasize that this phase instability only occurs along the solid-fluid interface which has a constant normal stress. The other interfaces of this non-hydrostatically stressed solid will have different equilibrium conditions.

4.2.2. Solid-solid case

In the solid-solid case, both polymorphs experience non-hydrostatic stresses (Figure 1a) which allows for different stability behaviors (Figure 2). In the solid-fluid case, as Sekerka and Cahn (2004) showed, the hydrostatically stressed "fluid" will always be stable relative to the non-hydrostatically stressed solid. In the solid-solid case, however, it is possible to have different critical point stabilities (i.e., isothermal surface topologies) depending on the relative elastic constants of the solids. Figure 4 illustrates the possible isothermal surface topologies different polymorph pairs may have by plotting elastic moduli combinations for hypothetical isotropic polymorph pairs. This allows for the characterization of possible polymorph pair responses to stress variation.

The ratio of the Young's moduli of the high-pressure phase relative to the low-pressure phase determines the stability of each phase with variation in the interface-parallel stresses 2 and 3 under constant normal stress (Figure 4). This is because Young's modulus is a measure of the stiffness of a material. The higher the Young's modulus of a solid, the less strain energy will be imparted by stress variation, making it more stable relative to solids with lower Young's moduli. When the ratio of the Young's moduli is low, the behavior is the same as in the solid-fluid case:

any interface-parallel stress variation will cause the low-pressure phase to become stable relative to the high-pressure phase because the isothermal surfaces are concave up (Figure 4 sections I and IV). In contrast, when the ratio of the Young's moduli is high, any interface-parallel stress variation will cause the high-pressure phase to be stable relative to the low-pressure phase as the isothermal surfaces are now concave down (Figure 4 sections III and VI).

Poisson's ratio adds further complexity. The Poisson's ratio characterizes how applied stress on one axis causes deformation on the others. If the Poisson's ratios are equal between the phases, the stability will simply shift from a concave-up surface to a concave-down surface at a single point as the Young's moduli ratio increases. However, if the Poisson's ratios are different, the stability transition will be more complex, and the isothermal surface will become a saddle surface as the stability transition occurs (Figure 4, sections II and V). In this case, either the high-pressure or the low-pressure phases could be more stable depending on the variations in stresses 2 and 3. Lastly, the relative Poisson's ratios determine the orientation and eccentricity of the elliptical cross sections of the surfaces. The transition between ellipse orientations is shown in Figure 4 by the dashed line.

4.2.3. High-pressure polymorph stability with stress decrease

High-pressure polymorphs typically have higher Young's moduli than low-pressure polymorphs. Consequently, in the solid-solid case (Figure 1a), the Al_2SiO_5, C, and $CaCO_3$ polymorph pairs all have isothermal surfaces that correspond to section VI of Figure 4 (Figures 1b, 2a, and 2b). In this case, the high-pressure polymorphs will be stable relative to the low-pressure polymorphs with interface-parallel stress variations away from hydrostatic equilibrium. The SiO_2 polymorph pair is an exception because of quartz's low Poisson's ratio (Pabst & Gregorova, 2013). But the SiO_2 polymorphs aside, the stability of high-pressure polymorph

interfaces with interface-parallel stress variation has an unexpected and profound implication: a *decrease* in stress can make a high-pressure polymorph *more* stable at a given interface (Figure 5).

Consider a graphite crystal that is hydrostatically stressed at -3.3 GPa (compressive stress is negative by convention) at a temperature of 643 ^{o}C, placing it just below the boundary of graphite/diamond equilibrium (Figures 2a and 5a). If the stress on one of the axes of the graphite crystal decreases while the temperature is held constant, then the diamond would become more stable than graphite on the interfaces normal to the unchanged stress (Figures 5b and 5c). This unintuitive result means that a drop in stress in a geological system could allow for the formation of a higher-pressure phase on certain interfaces parallel to the stress decrease (Figure 5c). Thus, although interface equilibrium temperatures are relatively insensitive to interface-parallel stress variations, these stress variations still have important effects on the stability of interfaces at or near equilibrium.

4.3. Application to natural systems

The predicted effects of non-hydrostatic stress on phase stability must be applied to natural systems with care as many factors will affect the thermodynamic relationships.

4.3.1. Fluid-bearing systems

One of the most important considerations is the presence of a fluid phase. Fluids may diminish or circumvent predicted variations in mineral stability in a non-hydrostatically stressed system because fluids have a constant pressure at equilibrium (Figures 6a and 6b). Since many metamorphic reactions are mediated by pore fluids, the fluid pressure would dictate the equilibrium mineral assemblage for a fluid-bearing system with interconnected porosity (Figure 6a; Llana-Fúnez et al., 2012). Consequently, non-hydrostatic stress would likely change

436 equilibrium mineral assemblages by ~5 ^{o}C or less (Figure 1g). This is consistent with Bruton and
437 Helgeson (1983) and Powell et al. (2018).

438 Nonetheless, there could be variation in mineral equilibria in fluid-bearing systems if
439 there are isolated fluid pockets with different fluid pressures which can be considered to have
440 their own local equilibria (Larché & Cahn, 1978b; Figure 6b). This is a possibility at lower
441 crustal depths where fluids may form isolated pockets instead of interconnected networks due to
442 surface energy contrasts between the solids and fluids (Connolly & Podladchikov, 2004;
443 Holness, 1993; Yoshino et al., 2002). Moore et al. (2019) report the preservation of such grain-
444 scale variations in local mineral equilibria in shear zones.

445 **4.3.2. Dry systems**

446 Dry systems which lack a fluid phase do not have these same restrictions because elastic
447 solids can sustain non-hydrostatic stresses at equilibrium. This makes the effects of non-
448 hydrostatic stress on interface equilibrium and consequent equilibrium assemblages directly
449 applicable.

450 **4.3.2.1. Irreversible deformation**

451 One must first consider whether solids in the system can be treated as elastic. If energy-
452 dissipating processes such as irreversible deformation (e.g., plastic, ductile, or viscous) are
453 occurring, the solids become fluid-like in behavior making the application of solid
454 thermodynamics difficult (Figure 6c; Hobbs & Ord, 2016, 2017). These dissipative processes are
455 functions of many geologic variables including temperature, differential stress, mineral strength,
456 dissolved hydrogen content, and grain size (e.g., Kohlstedt et al., 1995; Karato & Jung, 2003).
457 However, on short enough timescales, even irreversibly deforming solids can be approximated as
458 elastic, allowing the direct application of solid thermodynamics (e.g., Moulas et al., 2019).

4.3.2.2. Elastic solids and stress limiting reactions

The non-hydrostatic equilibrium thermodynamic relationships discussed in this paper are directly applicable to dry systems (i.e., no free fluid phase) in which the solids can be approximated as elastic on the timescale relevant to the evolution of the metamorphic system. In such situations, chemical equilibrium conditions for single-component elastic solid interfaces can be directly calculated using equation (10).

While non-hydrostatic stress may lead to changes in mineral stability with orientation, dry systems without significant dissipative processes still have a mechanism by which they can limit the effect of non-hydrostatic stress on mineral assemblages: the large volume changes associated with polymorphic reactions (Ferry, 2000). The molar volume decreases associated with the four low-to-high pressure polymorph reactions in this study are 7.4% ($CaCO_3$), 9.0% (SiO_2), 11.5% (Al_2SiO_5), and 58.5% (C) at 25 ^oC and 10^5 Pa (Holland & Powell, 2011). In elastic strain theory, a volume change of several percent typically requires multiple GPa of pressure variation. This means that polymorphic reactions in rocks such as quartzites and marbles can act to limit non-hydrostatic stress, depending on the timescales of compaction and relaxation.

For example, consider a hypothetical aggregate of calcite and aragonite in a fixed volume at a constant temperature as in Figure 6d where the maximum stress is above the calcite/aragonite reaction boundary and the minimum stress is below the boundary. Calcite, the low-pressure polymorph, will break down to form aragonite, the high-pressure polymorph, on interfaces normal to the maximum stress. The aragonite may then grow parallel to the maximum stress (Hacker & Kirby, 1993; Vaughan et al., 1984). This will cause the volume to decrease in the direction of the maximum stress, lowering the maximum stress down to the calcite/aragonite reaction boundary. Likewise, we predict that aragonite will break down to form calcite on

interfaces normal to the minimum stress, and the calcite will then grow parallel to the minimum stress. This would increase the volume, raising the stress to the calcite/aragonite reaction boundary. Consequently, both the maximum and minimum stresses in the system will tend toward the calcite/aragonite reaction boundary, diminishing non-hydrostatic stress.

However, in real systems the volume is not constant, and the rate of compaction or relaxation will serve to increase or decrease stresses, respectively, limiting the timescale on which the non-hydrostatic stresses may be diminished. We also note that there may be other factors which influence mineral shape-preferred orientations. If both stresses lie within one of the polymorph's stability fields or if mineral growth kinetics are complex or anisotropic, growth parallel to the maximum or minimum stress may not be realized. Future work is clearly needed to investigate the interactions of kinetics and thermodynamic driving force. Additionally, it is worth noting that any numerical model that attempts to determine the grain-scale stresses in a system with polymorphic reactions must account for these large volume changes; this may pose difficulties for classical continuum modeling approaches.

An important implication of these large reaction volume changes is that by potentially limiting stresses near reaction boundaries, interface-parallel stresses may become more relevant to polymorphic reactions. When stresses are at or near equilibrium, the variations in interface-parallel stresses can make one phase unstable relative to the other (e.g., Figure 5). This could be important for settings with large, transient differential stresses such as in shear zones.

4.3.3. More complex fluid behavior

We have limited our discussion thus far to direct solid-fluid (Fig. 6a and 6b) and solid-solid reactions (Fig. 6d). These reactions are relatively simple and the thermodynamic behaviors indicated by our results have strong experimental support (e.g., Llana-Fúnez et al., 2012; Richter

et al., 2016). However, there are additional reaction pathways that are not captured in Figure 6 which may operate in geological systems (e.g., Wheeler, 2014). These include reaction phenomena involving fluid films which sustain stress (Alcantar et al., 2003; Bernabé & Evans, 2014; Correns, 1949 Dahlen, 1992; Kristiansen et al., 2011; Rutter, 1983) and constant-volume interface-coupled dissolution-reprecipitation reactions (e.g., Ague & Axler, 2016; Putnis & Austrheim, 2010; Putnis & John, 2010). The interactions between non-hydrostatic stress, solids, and fluids are more complex in these scenarios and are not as well understood as direct solid-solid or solid-fluid reactions. Consequently, we leave these phenomena as topics for future work.

4.3.4. Evidence of non-hydrostatic stress in preserved assemblages

Normal stress determines an interface's chemical potential and consequent stability to first order at a fixed temperature. Consequently, for polymorphic reactions, high-pressure phases will nucleate normal to the maximum stress (Cionoiu et al., 2019; Green & Burnley, 1989; Hacker & Kirby, 1993; Kirby et al., 1991; Richter et al., 2016; Schubnel et al., 2013; Vaughan et al., 1984; Figure 3c) and then may grow parallel to the maximum stress (Hacker and Kirby, 1993; Vaughan et al., 1984). Similarly, we predict that low-pressure phases will nucleate normal to the minimum stress and then grow parallel to the minimum stress. Thus, we postulate that the preservation of phase orientations relative to principal stress directions could be an important indicator of non-hydrostatic stress influencing the thermodynamic and kinetic development of a mineral assemblage.

These orientations could easily be interpreted to be a result of (and could be coupled with) mechanical forces that influence mineral shape and crystallographic preferred orientations and rock fabrics. Future work will be needed to determine the relative influences of these processes. For example, on Syros, Greece, oriented pseudomorphs of calcite after aragonite are

widespread. Their long axes and *c*-axes are oriented parallel to the inferred maximum stress. The calcite is almost certainly a topotactic replacement of the aragonite, preserving the original aragonite shape and crystallographic orientation (Brady et al., 2004; Carlson & Rosenfeld, 1981). The crystallographic preferred orientation has previously been interpreted to be a result of dislocation creep (Brady et al., 2004). However, the pseudomorphs lack evidence of dynamic recrystallization, and their shape-preferred orientation is inconsistent with a dislocation creep mechanism (Rybacki et al., 2003). On the other hand, the observed orientations are fully consistent with the predicted effects of non-hydrostatic stress on shape preferred (Figure 6d) and crystallographic preferred orientations (Kamb, 1959). Consequently, we speculate that these marbles may instead be an example of non-hydrostatic stress influencing mineral stability and consequent polymorphic phase transformations and growth.

4.4. Implications for the evolution of non-hydrostatically stressed dry mineral assemblages

Non-hydrostatic stress is predicted to have significant effects on mineral assemblages in dry lithospheric systems where the solids behave elastically on the timescale of interest. Polymorphic mineral assemblages in rocks such as quartzites, marbles, and peridotites in cold, stressed subduction zones may therefore be ideal for the direct application of the concepts developed herein. However, any mineral assemblage in which solid-solid reactions are occurring could potentially be relevant.

Chemical potential and consequent phase stability depend primarily on the normal stress on an interface (Figures 1 and 2). Therefore, non-hydrostatic stress not only influences the shape and potentially the crystallographic preferred orientations (Kamb, 1959) of polymorphic mineral assemblages as previously discussed, but it also controls the thermodynamic driving force behind such reactions. Consequently, we suggest that the normal stress on each interface should be used

when modeling reaction kinetics, as we explore further below. Using the correct stresses for thermodynamic and kinetic calculations in non-hydrostatically stressed systems will allow for both better understanding and modeling of geological processes.

4.4.1. Phase changes and reaction kinetics

Non-hydrostatic stress will result in the preferential orientation of polymorphic reactions. The spatial alignment of polymorphic reactions has implications for transient processes in metamorphic and mantle systems, including seismicity. For example, polymorphic reactions between nominally dry olivine, wadsleyite, and ringwoodite are proposed as a mechanism for the initiation of deep-focus earthquakes that occur at depths of approximately 400 to 700 km (e.g., Kirby et al., 1996). The olivine to wadsleyite reaction occurs at about 410 km depth, and the wadsleyite to ringwoodite reaction occurs at about 520 km depth; however, the reactions are typically overstepped inside cold subducting slabs (e.g., Green & Houston, 1995) which would lead to the range of observed earthquake depths.

This mechanism, termed transformational faulting, has been tested experimentally through the analogue material Mg_2GeO_4 which is similar to olivine (Mg_2SiO_4) but reacts at lower pressures. Experiments have shown that the polymorphic reaction occurs on interfaces normal to the maximum stress (Green & Burnley, 1989; Schubnel et al., 2013; Vaughan et al., 1984). This is consistent with the thermodynamic analysis presented herein and other experiments of polymorphic reactions under stress (Figure 3; Hacker & Kirby, 1993; Hirth & Tullis, 1994; Kirby et al., 1991; Richter et al., 2016; Zhou et al, 2005). The polymorphic reactions create "anticracks" from the volume decrease, which are oriented normal to the maximum stress and comprise small grains of the high-pressure polymorph. These anticracks self-organize into faults that generate seismic slip due to superplastic flow (Green & Burnley, 1989). Transformational

faulting could result from other polymorphic reactions such as quartz/coesite, calcite/aragonite, and clinoenstatite/$MgSiO_3$ ilmenite structure. While this remains to be experimentally verified (e.g., Hacker & Kirby 1993), there is insufficient evidence to eliminate the possibility as some have suggested because experimental data is limited, and the high strains in experiments don't necessarily accurately reflect slow geological processes (Karato, 2010).

The influence of non-hydrostatic stress extends beyond the orientation of polymorphic reactions. Non-hydrostatic stress also influences reaction kinetics, and the appropriate stresses should be used for these calculations. Transformational faulting in deep-focus earthquakes, for example, depends on the existence of metastable olivine cores (or wedges; e.g., Kirby et al., 1996; Mosenfelder et al., 2001) in fast subducting slabs that allow for olivine reactions to overstep equilibrium and occur deeper than they typically would in the mantle (Green & Houston, 1995). Consequently, there is great interest in experimentally constraining the reaction kinetics between olivine, wadsleyite, and ringwoodite (e.g., Kerschhofer et al., 1998; Mosenfelder et al., 2001; Rubie and Ross, 1994). Reaction kinetics from such studies have been used to constrain models for both the extent of metastable olivine wedges in subducting slabs and the occurrences of transformational faulting that may generate deep earthquakes (e.g., Devaux et al., 1997; Kirby et al., 1996; Mosenfelder et al., 2001). These models use constant pressures in their calculations. However, metastable olivine wedges may have differential stresses that exceed 1 GPa (Devaux et al., 2000). Such a large stress differential would lead to significantly different results for metastable olivine wedge models depending on what stress was used for the pressure term of the reaction kinetics. We have shown that normal stress determines chemical potential and consequent phase stability to first order (Figures 1 and 2) as corroborated by experimental evidence (Richter et al., 2016; Vaughan et al., 1984; Figure 3). Therefore, we

posit that models should use the appropriate normal stress value. In this case, since the high-pressure phases nucleate normal to the maximum compressive stress, we suggest that the maximum stress value should be used as it is the greatest thermodynamic driving force for the reaction.

Beyond deep earthquakes, all reactions occurring under non-hydrostatic stress should be modeled using the appropriate normal stress values in equations for phase stability and reaction kinetics. Using an averaged value such as mean stress instead will lead to incorrect determinations of local mineral stability on the grain scale and to incorrect estimations of the maximum thermodynamic driving force for overstepped reactions on the regional scale.

The full effects of non-hydrostatic stress on reaction kinetics can be calculated in a similar way to how they were for chemical potential and phase stability in equation (10); however, in many cases this may not be necessary. As with Helmholtz free energy (A), non-hydrostatic internal energy (E) is also function of strain energy which can be calculated with equation (6). The volume change can be calculated using equation (8). Together, these can be used to calculate any molar enthalpy (H) terms often involved in kinetic rates (e.g., Rubie & Ross, 1994). However, since change in strain energy is orders of magnitude smaller than the corresponding change in stress, incorporating these changes will likely alter results by 1% or less (e.g., Figure 1c). Consequently, in most cases simply replacing pressure terms, such as in equation (1), with normal stress is an appropriate approximation of a full calculation such as in equation (10) (e.g., Ferry, 2000). This means that the effects of non-hydrostatic stress on mineral stability and reaction kinetics can be easily and more accurately obtained so long as the appropriate normal stress value is used in thermodynamic equations as in the example of deep earthquakes.

4.4.2. Metamorphic fabrics and volume change

The mechanical controls of non-hydrostatic stress on shape and crystallographic preferred orientation through deformation have been extensively investigated (e.g., Wenk, 1985). However, there may be thermodynamic controls on metamorphic fabrics that have yet to be explored. After nucleation, non-hydrostatic stress will likely influence both the shape and crystallographic preferred orientation of polymorphs as they grow (e.g., Brady et al., 2004; Hacker & Kirby, 1993; Kamb, 1959; Vaughan et al., 1984). As most polymorphs are structurally anisotropic, thermodynamically-induced preferred orientations may alter regional rheology and may create seismic anisotropy (e.g., Brocher & Christensen, 1990; McNamara et al., 2002).

Additionally, the volume change associated with oriented polymorphic reactions could influence both the rock properties and surrounding lithologies. For example, directional volume decreases within a rock from orientated reactions may lead to the development of channelized porosity (e.g., Jamtveit et al., 2000; Plümper et al., 2017). This may create efficient pathways for the initiation of fluid infiltration in, for example, subducting marbles and carbonate-bearing silicate rocks. Such infiltration, in turn, could have important geochemical implications, as fluid-driven decarbonation reactions and the stoichiometric dissolution of $CaCO_3$ are important contributors of CO_2 to the geologic carbon cycle (e.g., Ague & Nicolescu, 2014; Kelemen & Manning, 2015; Kerrick & Connolly, 2001; Stewart & Ague, 2020).

Volume changes may also lead to regional deformation. Polymorphic mineral assemblages in rocks such as marbles may be subducted, leading to high-pressure polymorph formation followed by exhumation and subsequent low-pressure polymorph formation (e.g., Brady et al., 2004; Chopin, 1984; Peterman et al., 2009). The large volume changes associated with these polymorphic reactions on both burial and exhumation paths may lead to deformation

643 of adjacent rocks and could possibly affect surface uplift and subsidence (Iyer and Podladchikov,
644 2009; Peterman et al., 2009).

645 **5. Conclusion**

646 Understanding the interplay of non-hydrostatic stress and the chemical evolution of
647 metamorphic systems is critical for investigating processes in settings such as subduction zones
648 and orogenic wedges. To the extent that minerals can be approximated as elastic solids, non-
649 hydrostatic thermodynamic theory as derived by Larché and Cahn (1973; 1978a, 1978b, 1985)
650 can be used to help understand how non-hydrostatic stress influences processes such as phase
651 stability, reaction kinetics, deformation, and seismicity.

652 The application of Larché-Cahn theory to polymorphic reactions indicates that at a fixed
653 temperature, normal stress determines the chemical potential, and therefore stability, of each
654 phase on a given interface to first order. In contrast, the influence of interface-parallel stresses on
655 an interface's chemical potential is approximately two orders of magnitude smaller. Thus, we
656 suggest that normal stress should be used for calculations of phase stability and reaction kinetics.
657 Nonetheless, interface-parallel stress variations allow for the surprising possibility that a stress
658 decrease in a low-pressure polymorph that is near a polymorphic reaction boundary can lead to
659 the formation of the high-pressure polymorph.

660 These concepts are directly applicable to dry systems with elastic solids that can sustain
661 non-hydrostatic stresses at equilibrium. Under dry conditions, the control of normal stress on
662 interface stability predicts three effects on polymorphic reactions. First, high-pressure
663 polymorphs should form when the maximum stress exceeds the pressure of the phase transition,
664 and low-pressure polymorphs, when the minimum stress is less than the pressure of the
665 transition. Second, high-pressure polymorphs should nucleate normal to the maximum stress, and

low-pressure polymorphs, the minimum stress. Finally, high-pressure polymorphs may grow parallel to the maximum stress, and low-pressure polymorphs, the minimum stress. The resulting shape and crystallographic preferred orientations of polymorphic reactions under non-hydrostatic stress may be especially important in the evolution of monomineralic polymorphic assemblages in rocks such as quartzites, marbles, and peridotites. Polymorphic phase transitions under non-hydrostatic stress have been shown to generate seismicity. They may additionally influence seismic anisotropy, rock porosity, and local and regional deformation. Thus, non-hydrostatic stress has a rich variety of effects on the evolution of geological systems that have yet to be fully described, quantified, or potentially even discovered.

Acknowledgements:

We thank J. Wheeler and an anonymous reviewer for their insightful comments on the manuscript, and L. Entwisle for help with figure design. Financial support from Yale University is gratefully acknowledged.

Data Availability Statement:

The thermodynamic dataset is from Holland and Powell (2011). Data were not created for this research

Figures

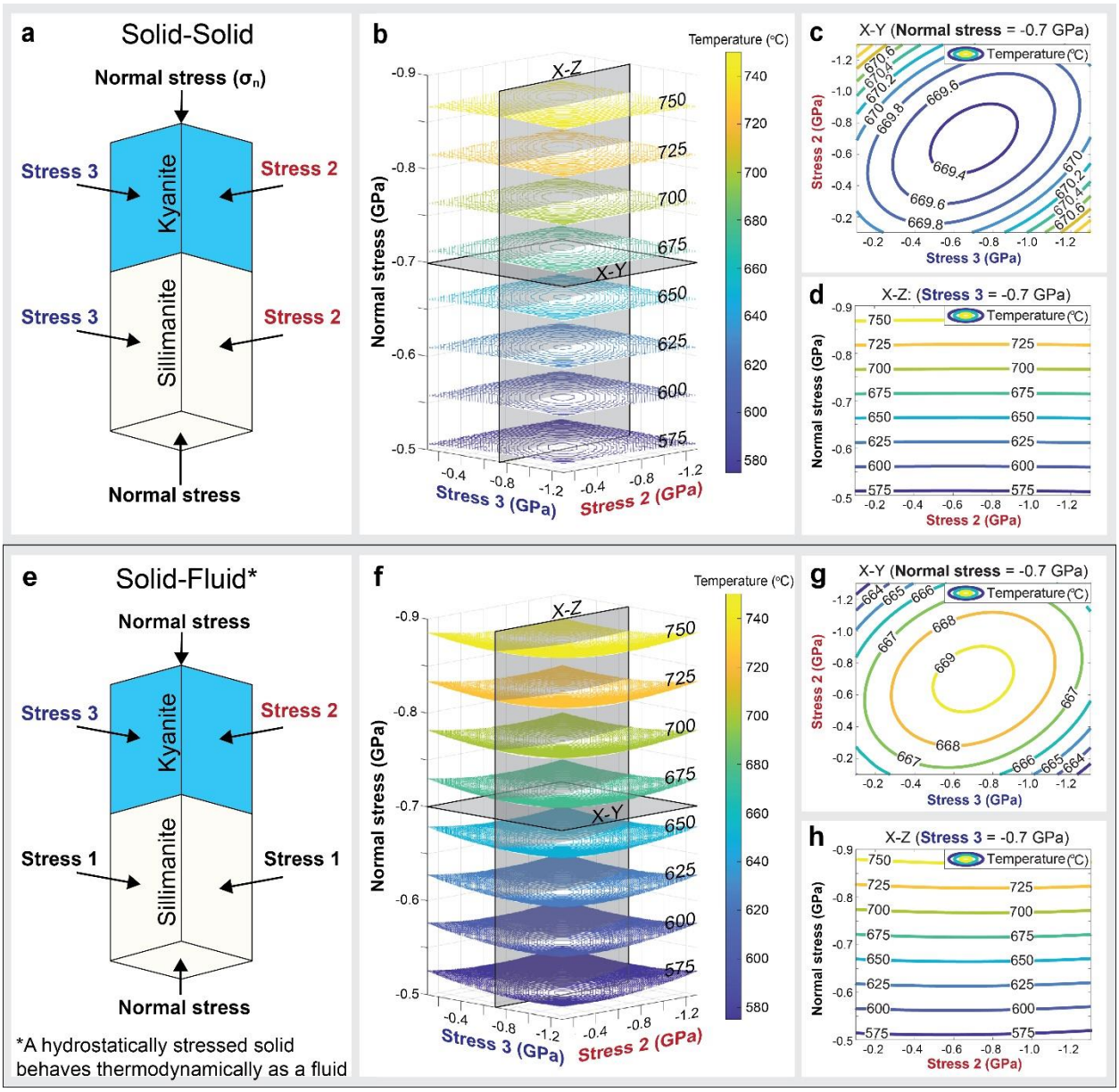

Figure 1. The magnitude of the effects of non-hydrostatic stress on solid-solid and solid-fluid interface equilibrium using the polymorphs kyanite and sillimanite. The hydrostatic reference frame equilibrium is -0.7 GPa and 667.4 °C (see Methods). We treat compressive stresses as negative. (a) Applied stress orientations for solid-solid kyanite and sillimanite equilibrium. The normal stress is normal to the considered interface while stresses 2 and 3 are parallel to the interface. (b) A contour plot of the equilibrium temperatures necessary for kyanite and sillimanite to co-exist at the interface shown in Figure 1a under a range of stress conditions. The

contours are isothermal surfaces which represent all stress combinations at which the interface is at equilibrium at the given temperature. (c) A cross section of Figure 1b where normal stress is held constant at -0.7 GPa while stresses 2 and 3 are varied. (d) A cross section of Figure 1b where stress 3 is held constant at -0.7 GPa while normal stress and stress 2 are varied. (e) Applied stress orientations for solid-fluid kyanite and sillimanite equilibrium. Sillimanite is hydrostatically stressed, representing a fluid. Stress 1 is equivalent to the normal stress. (f) A contour plot of the equilibrium temperatures necessary for kyanite and sillimanite to co-exist at the interface shown in Figure 1e. (g) A cross section of Figure 1f where normal stress is held constant at -0.7 GPa while stresses 2 and 3 are varied. (h) A cross section of Figure 1f where stress 3 is held constant at -0.7 GPa while normal stress and stress 2 are varied.

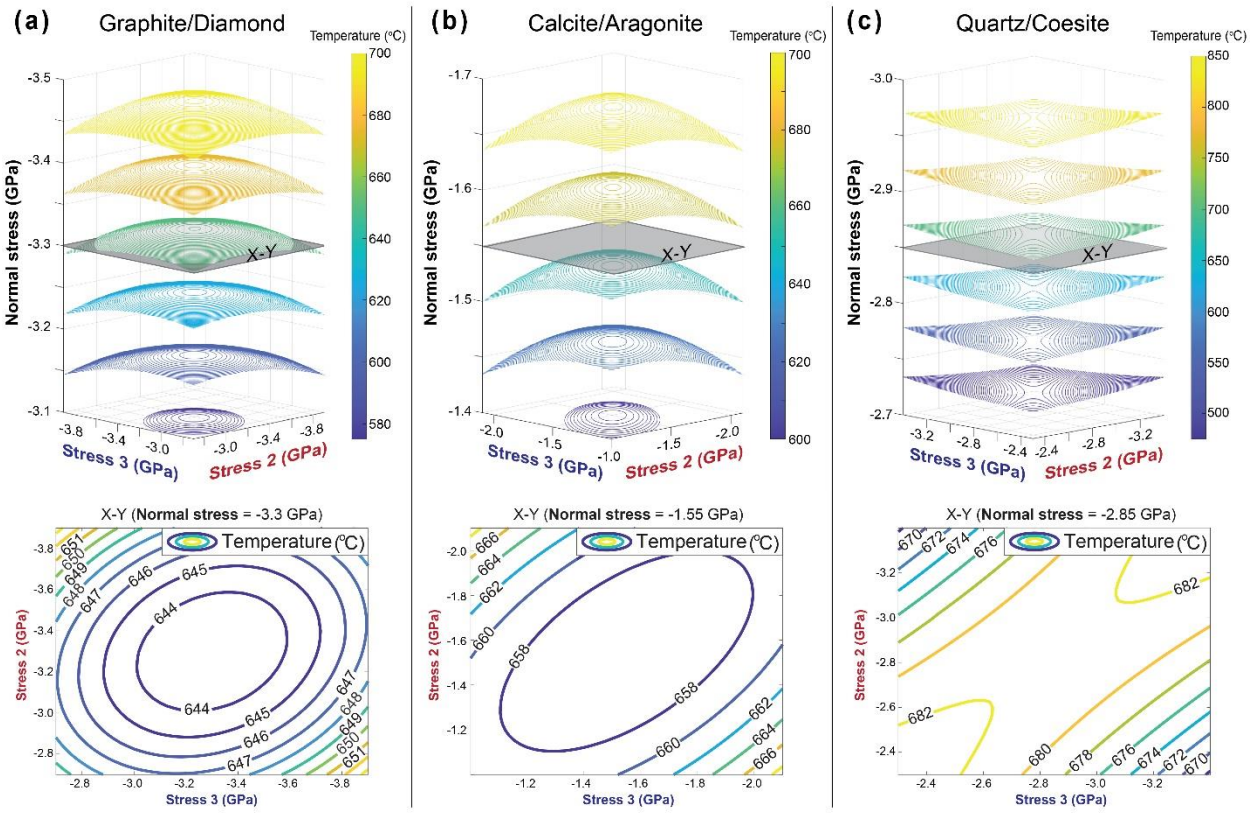

Figure 2. Interface equilibrium conditions for the polymorph pairs graphite/diamond (C), calcite/aragonite ($CaCO_3$), and quartz/coesite (SiO_2) using the same setup as Figure 1a. The top plots show equilibrium isothermal surfaces for the specified interface for a range of stress values. The isothermal surfaces show the possible stress values at which the given interface is at equilibrium for the given temperature. The bottom plots are cross sections at a fixed normal stress. The contours show the equilibrium temperature of the given interface at different values of stresses 2 and 3 (i.e., interface-parallel stresses). (a) Graphite and diamond (C). (b) Calcite and aragonite ($CaCO_3$). (c) Quartz and coesite (SiO_2).

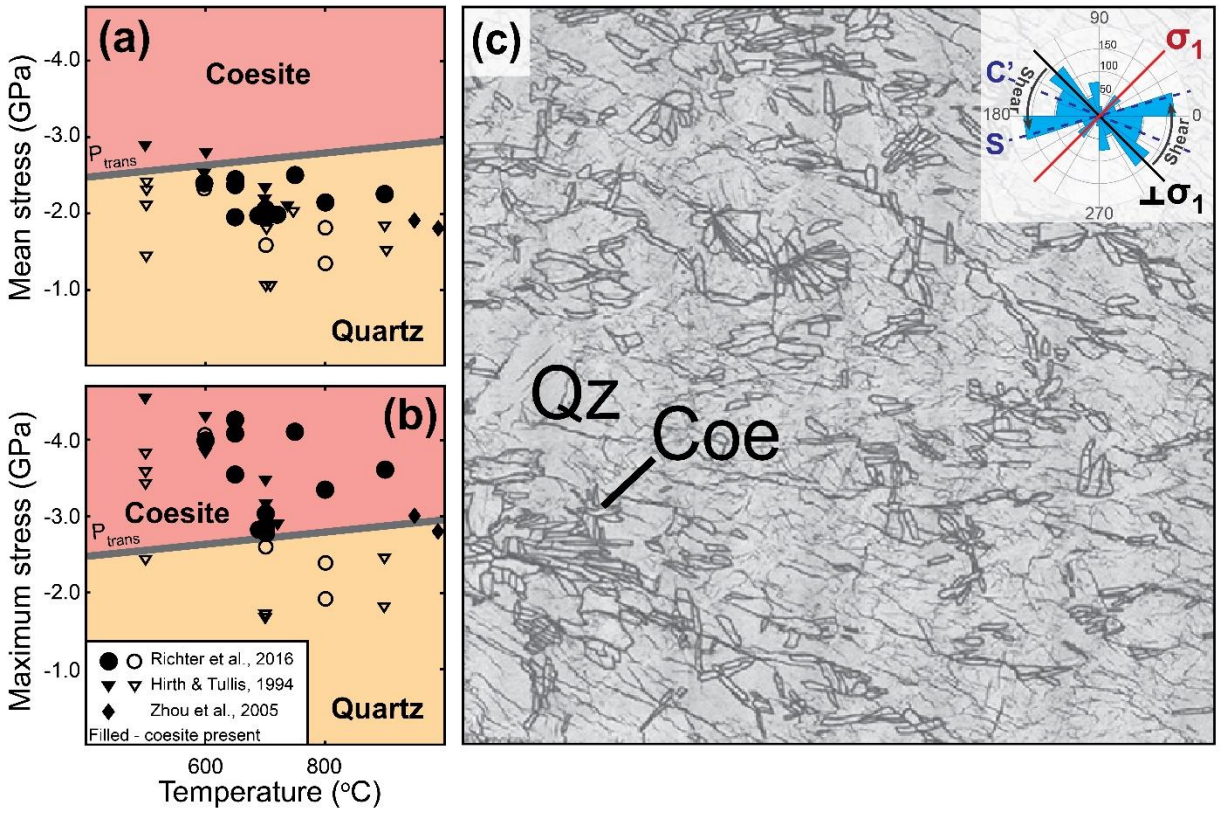

Figure 3. Quartz (Qz) uniaxial deformation experiments which formed coesite (Coe) using a modified Griggs apparatus. Figure modified after Richter et al. (2016). (a) The mean stress

718 $\left(\frac{\sigma_1+\sigma_3+\sigma_3}{3}\right)$ plotted against the temperature for the given experiments where σ_1 is the maximum
719 stress and σ_3 is the minimum stress (i.e., the confining pressure). The gray line denotes the
720 pressure of the transition between quartz and coesite under hydrostatic stress conditions after
721 Bohlen and Boettcher (1982). The filled symbols are the experiments in which coesite formed.
722 Most experiments which formed coesite have a mean stress below the pressure of transition
723 (P_{trans}) line, demonstrating that mean stress does not control the reaction. (b) The maximum
724 stress plotted against the temperature. The presence of coesite correlates strongly with maximum
725 stress exceeding the pressure of transition. (c) Scanning electron microscope image of coesite in
726 deformed sample 435br after Richter et al., 2016. Field of view is 650 μm. We created the inset
727 rose diagram by measuring the angles of the long axes of the coesite grains. The resulting
728 measurements indicate that the coesite grains nucleate on interfaces normal to the maximum
729 stress ($\perp\sigma_1$) and are rotated by progressive shearing into the shear (C') and foliation (S) planes.
730

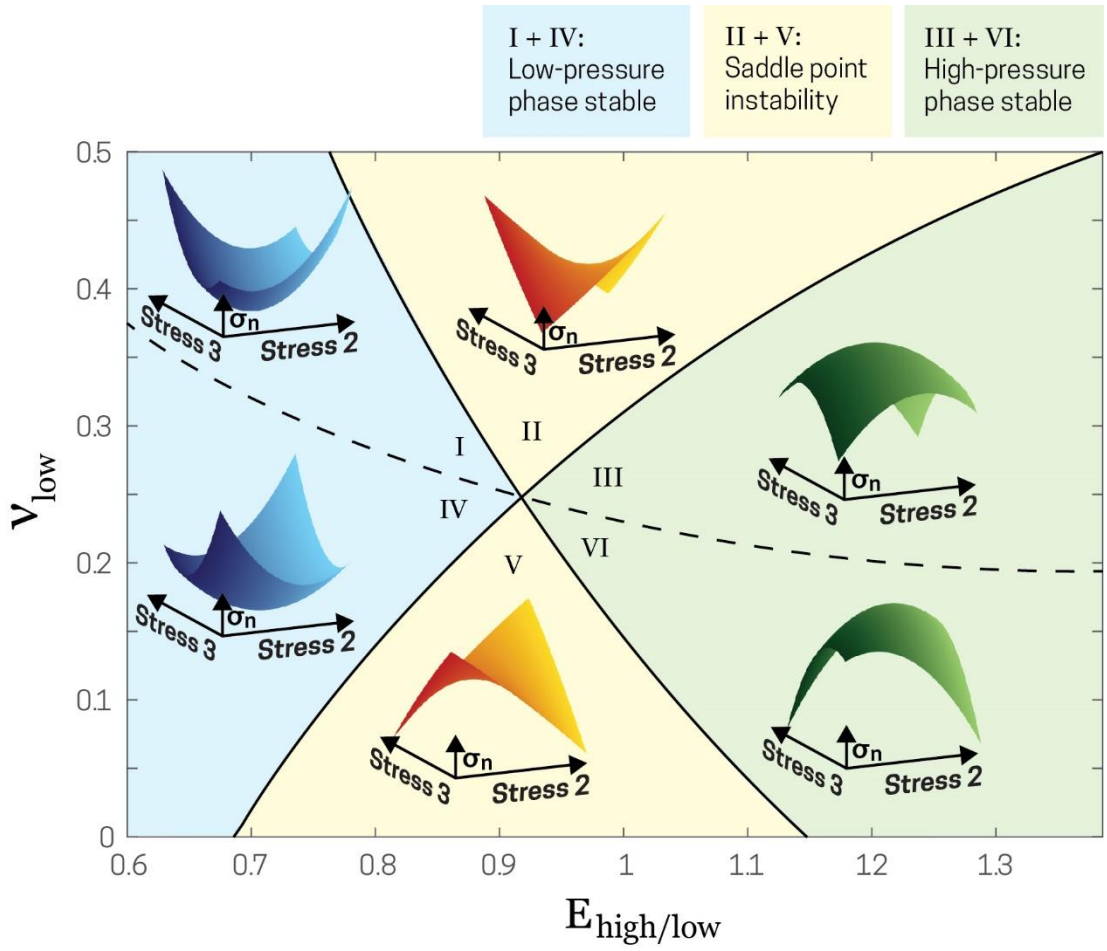

731

732 **Figure 4.** A stability diagram of isothermal surfaces with interface-parallel stress variations
733 based on different combinations of Young's moduli and Poisson's ratios for a hypothetical
734 isotropic high- and low-pressure polymorph pair. The high-pressure polymorph's Poisson's ratio
735 is fixed at 0.25. The x-axis is the ratio of the Young's modulus of the high-pressure polymorph
736 relative to the low-pressure polymorph ($E_{high/low}$), and the y-axis is the Poisson's ratio of the low-
737 pressure polymorph (ν_{low}). The surfaces are qualitative isothermal surfaces (see Figures 1 and 2).
738 The critical points (minima, maxima, or saddle points) are the hydrostatic stress value. In
739 sections I and IV the low-pressure polymorph is stable with stress 2 and 3 variations; in sections
740 II and V, there is a saddle point which means either could be stable; and in sections III and VI,

the high-pressure polymorph is stable. The dashed line indicates a change in the orientation of the surfaces.

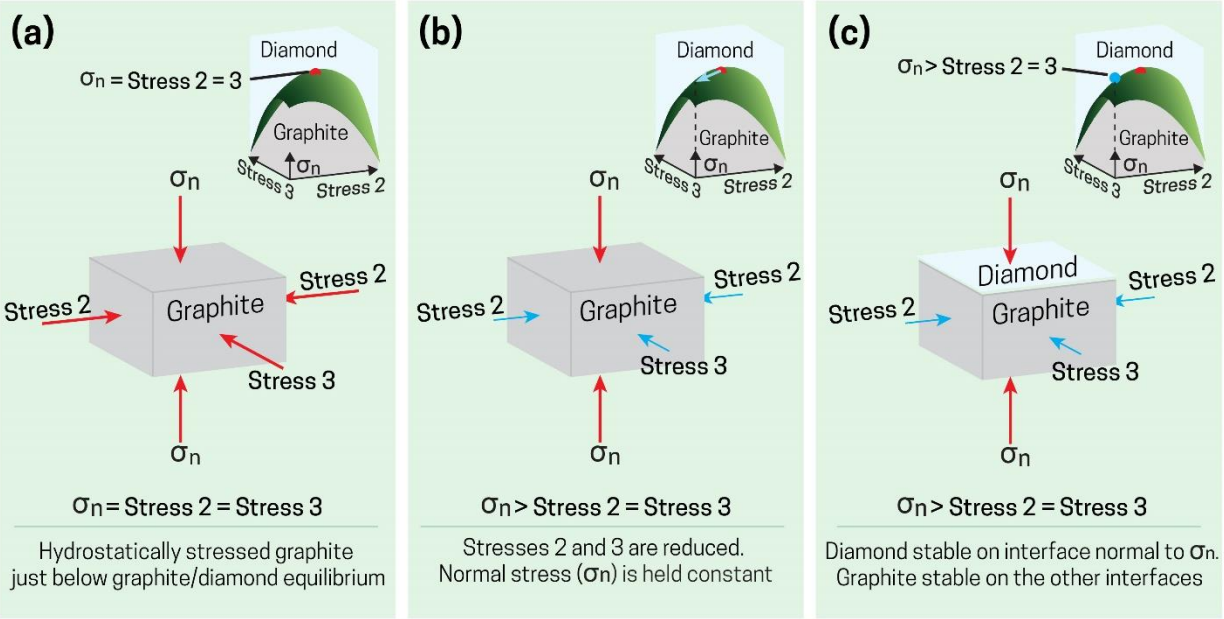

Figure 5. The effects of stress variation on polymorphs near equilibrium. (a) Graphite is hydrostatically stressed just below graphite/diamond equilibrium. The inset plot (top right) shows the qualitative isothermal surface for the graphite/diamond equilibrium on the interface normal to the normal stress (σ_n; see Figures 2 and 4). (b) Stresses 2 and 3 are decreased while the normal stress and system temperature are held constant. The blue arrow in the inset plot shows the change in interface stability. (c) The interface normal to the normal stress is now more stable as diamond than graphite because the stress on the interface falls in the diamond stability field (blue dot in the inset plot). Graphite remains stable on the interfaces normal to stresses 2 and 3. This demonstrates how a stress decrease in a system can make a high-pressure polymorph such as diamond more stable.

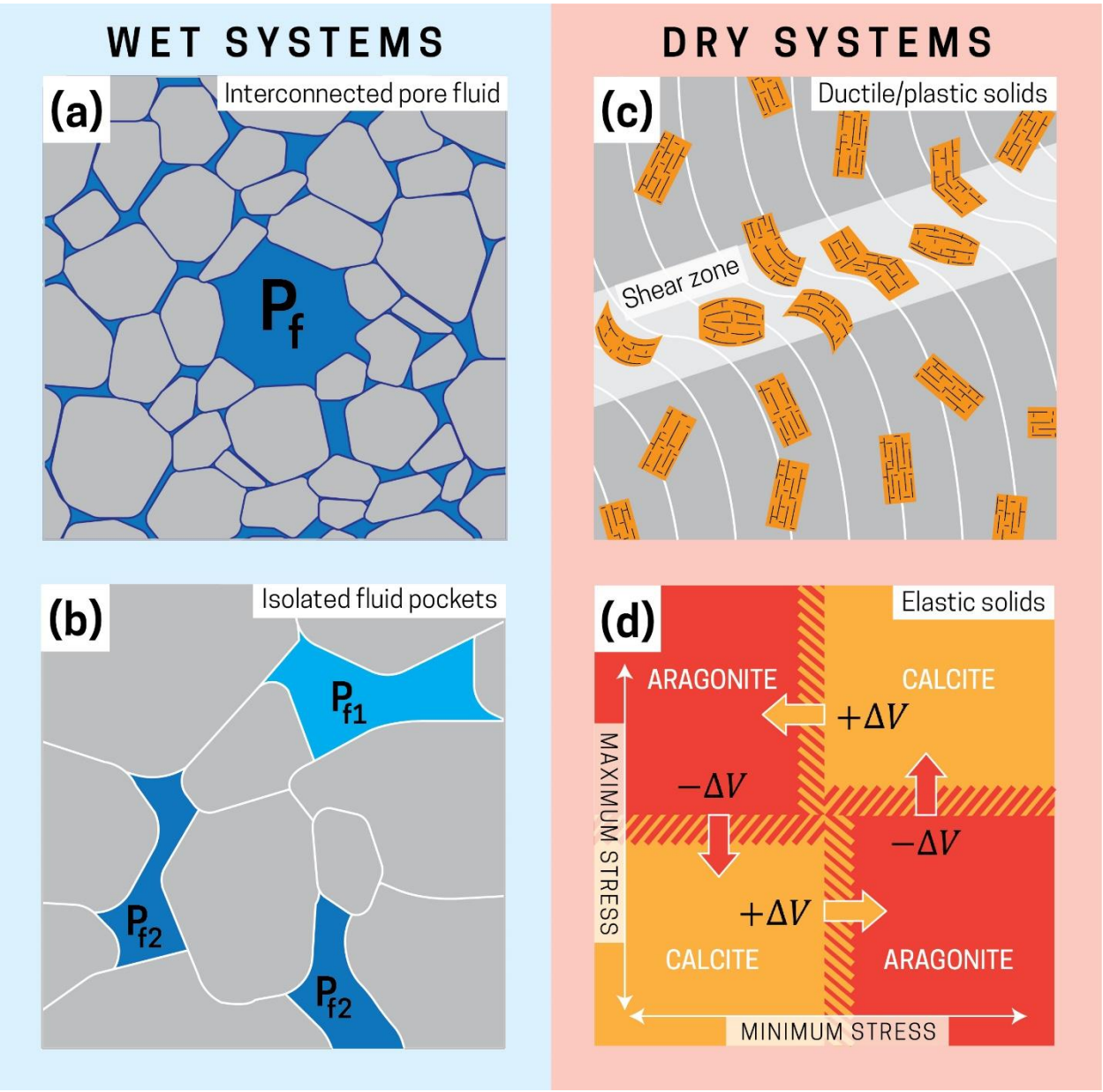

Figure 6. Controls on mineral equilibria for metamorphic systems with direct solid-fluid and solid-solid reactions. Wet systems: (a) In systems with interconnected pore fluids that mediate chemical reactions, the equilibrium mineral assemblages will be determined by the fluid pressure (P_f) which will be constant in each system. (b) In systems with isolated fluid pockets at different pressures (P_{f1} and P_{f2}) equilibrium mineral assemblages will be determined locally by each fluid pressure. This could locally preserve different pressure mineral assemblages. Dry systems: (c)

Minerals undergoing plastic and ductile deformation. Under these conditions, the application of equilibrium thermodynamics is complicated as the solids act as viscous fluids in disequilibrium. White lines represent foliation in a rock with a shear zone where orange minerals are being deformed. (d) Minerals that behave as elastic solids. Normal stress on each interface controls phase stability. The maximum stress is in the aragonite stability field, and the minimum stress is in the calcite stability field. Large volume changes (ΔV) associated with metamorphic reactions could diminish non-hydrostatic stresses.

References:

Ague, J. J., & Axler, J. A. (2016). Interface coupled dissolution-reprecipitation in garnet from subducted granulites and ultrahigh-pressure rocks revealed by phosphorus, sodium, and titanium zonation. *American Mineralogist, 101*(7), 1696-1699. https://doi.org/10.2138/am-2016-5707

Ague, J. J., & Nicolescu, S. (2014). Carbon dioxide released from subduction zones by fluid-mediated reactions. *Nature Geoscience,* 7, 355-360. https://doi.org/10.1038/ngeo2143

Alcantar, N., Israelachvili, J., & Boles, J. (2003). Forces and ionic transport between mica surfaces: Implications for pressure solution. *Geochimica et Cosmochimica Acta, 67*(7), 1289-1304. https://doi.org/10.1016/S0016-7037(02)01270-X

Andersen, T. B., Mair, K., Austrheim, H., Podladchikov, Y. Y., & Vrijmoed, J. C. (2008). Stress release in exhumed intermediate and deep earthquakes determined from ultramafic pseudotachylyte. *Geology, 36*(12), 995-998. https://doi.org/10.1130/G25230A.1

783 Bernabé, Y., & Evans, B. (2014). Pressure solution creep of random packs of spheres. *Journal of*
784 *Geophysical Research: Solid earth, 119*(5), 4202-4218.
785 https://doi.org/10.1002/2014JB011036
786 Bohlen, S. R., & Boettcher, A. L. (1982). The quartz ⇆ coesite transformation: A precise
787 determination and the effects of other components. *Journal of Geophysical Research:*
788 *Solid Earth, 87*(B8), 7073-7078. https://doi.org/10.1029/JB087iB08p07073
789 Brady, J. B., Markley, M. J., Schumacher, J. C., Cheney, J. T., & Bianciardi, G. A. (2004).
790 Aragonite pseudomorphs in high-pressure marbles of Syros, Greece. *Journal of*
791 *Structural Geology, 26*(1), 3-9. https://doi.org/10.1016/S0191-8141(03)00099-3
792 Brocher, T. M., & Christensen, N. I. (1990). Seismic anisotropy due to preferred mineral
793 orientation observed in shallow crustal rocks in southern Alaska. *Geology, 18*(8), 737-
794 740. https://doi.org/10.1130/0091-7613(1990)018<0737:SADTPM>2.3.CO;2
795 Bruton, C. J., & Helgeson, H. C. (1983). Calculation of the chemical and thermodynamic
796 consequences of differences between fluid and geostatic pressure in hydrothermal
797 systems. *American Journal of Science*, 283A, 540-588.
798 Carlson, W. D., & Rosenfeld, J. L. (1981). Optical determination of topotactic aragonite-calcite
799 growth kinetics: metamorphic implications. *The Journal of Geology, 89*(5), 615-638.
800 Chen, T., Gwanmesia, G. D., Wang, X., Zou, Y., Liebermann, R. C., Michaut, C., & Li, B.
801 (2015). Anomalous elastic properties of coesite at high pressure and implications for the
802 upper mantle X-discontinuity. *Earth and Planetary Science Letters, 412*(15), 42-51.
803 https://doi.org/10.1016/j.epsl.2014.12.025

Chopin, C. (1984). Coesite and pure pyrope in high-grade blueschists of the Western Alps: a first record and some consequences. *Contributions to Mineralogy and Petrology*, 86, 107-118. https://doi.org/10.1007/BF00381838

Christensen, N. I. (1996). Poisson's ratio and crustal seismology. *Journal of Geophysical Research, 101*(B2), 3139-3156. https://doi.org/10.1029/95JB03446

Cionoiu, S., Moulas, E., & Tajčmanová, L. (2019). Impact of interseismic deformation on phase transformations and rock properties in subduction zones. *Scientific reports*, 9, 19561. https://doi.org/10.1038/s41598-019-56130-6

Connolly, J. A. D. (2009). The geodynamic equation of state: What and how. *Geochemistry Geophysics, Geosystems, 10*(10). https://doi.org/10.1029/2009GC002540

Connolly, J. A. D., & Podladchikov, Y. Y. (2004). Fluid flow in compressive tectonic settings: Implications for midcrustal seismic reflectors and downward fluid migration. *Journal of Geophysical Research: Solid Earth*, 109, B04201. https://doi.org/10.1029/2003JB002822

Correns, C. W. (1949). Growth and dissolution of crystals under linear pressure. *Discussions of the Faraday society*, 5, 267-271.

Dahlen, F. A. (1992). Metamorphism of nonhydrostatically stressed rocks. *American Journal of Science, 292*(3), 184-198. https://doi.org/10.2475/ajs.292.3.184

Devaux, J. P., Fleitout, L., Schubert, G., & Anderson, C. (2000). Stresses in a subducting slab in the presence of a metastable olivine wedge. *Journal of Geophysical Research: Solid Earth, 105*(B6), 13365-13373. https://doi.org/10.1029/1999JB900274

Devaux, J. P., Schubert, G., & Anderson, C. (1997). Formation of a metastable olivine wedge in a descending slab. *Journal of Geophysical Research: Solid Earth, 102*(B11), 24627-24637. https://doi.org/10.1029/97JB02334

827 Ferry, J. M. (2000). Patterns of mineral occurrence in metamorphic rocks. *American*
828 *Mineralogist, 85*(11-12), 1573-1588. https://doi.org/10.2138/am-2000-11-1201
829 Gercek, H. (2007). Poisson's ratio values for rocks. *International Journal of Rock Mechanics*
830 *and Mining Sciences, 44*(1), 1-13. https://doi.org/10.1016/j.ijrmms.2006.04.011
831 Gibbs, J.W. (1875). On the equilibrium of heterogeneous substances. *Connecticut Academy of*
832 *Arts and Sciences Transactions,* 3, 108-248.
833 Gibbs, J.W. (1878). On the equilibrium of heterogeneous substances. *Connecticut Academy of*
834 *Arts and Sciences Transactions,* 3, 343–524.
835 Green, H. W. (1980). On the thermodynamics of non-hydrostatically stressed solids.
836 *Philosophical Magazine A, 41*(5), 637-647. https://doi.org/10.1080/01418618008239339
837 Green, H. W., & Burnley, P. C. (1989). A new self-organizing mechanism for deep-focus
838 earthquakes. *Nature*, 341, 733-737. https://doi.org/10.1038/341733a0
839 Green, H. W., & Houston, H. (1995). The mechanics of deep earthquakes. *Annual Review of*
840 *Earth and Planetary Sciences*, 23, 169-213.
841 Hacker, B. R., & Kirby, S. H. (1993). High-pressure deformation of calcite marble and its
842 transformation to aragonite under non-hydrostatic conditions. *Journal of Structural*
843 *Geology, 15*(9-10), 1207-1222. https://doi.org/10.1016/0191-8141(93)90164-6
844 Hirth, G., & Tullis, J. (1994). The brittle-plastic transition in experimentally deformed quartz
845 aggregates. *Journal of Geophysical Research, 99*(B6), 11731-11747.
846 https://doi.org/10.1029/93JB02873
847 Hobbs, B. E., & Ord, A. (2016). Does non-hydrostatic stress influence the equilibrium of
848 metamorphic reactions? *Earth-Science Reviews*, 163, 190-233.
849 https://doi.org/10.1016/j.earscirev.2016.08.013

Hobbs, B. E., & Ord, A. (2017). Pressure and equilibrium in deforming rocks. *Journal of Metamorphic Geology, 35*(9), 967-982. https://doi.org/10.1111/jmg.12263

Holland, T. J. B., & Powell, R. (2011). An improved and extended internally consistent thermodynamic dataset for phases of petrological interest, involving a new equation of state for solids. *Journal of Metamorphic Geology, 29*(3), 333-383. https://doi.org/10.1111/j.1525-1314.2010.00923.x

Holness, M. B. (1993). Temperature and pressure dependence of quartz-aqueous fluid dihedral angles: the control of adsorbed H_2O on the permeability of quartzites. *Earth and Planetary Science Letters, 117*(3-4), 363-377. https://doi.org/10.1016/0012-821X(93)90090-V

Iyer, K., & Podladchikov, Y. Y. (2009). Transformation-induced jointing as a gauge for interfacial slip and rock strength. *Earth and Planetary Science Letters, 280*(1-4), 159-166. https://doi.org/10.1016/j.epsl.2009.01.028

Jamtveit, B., Austrheim, H., & Malthe-Sørenssen, A. (2000). Accelerated hydration of the Earth's deep crust induced by stress perturbations. *Nature*, 408, 75-78. https://doi.org/10.1038/35040537

Kamb, W. B. (1959). Theory of preferred crystal orientation developed by crystallization under stress. *The Journal of Geology, 67*(2), 153-170.

Kamb, W. B. (1961). The thermodynamic theory of nonhydrostatically stressed solids. *Journal of Geophysical Research, 66*(1), 259-271. https://doi.org/10.1029/JZ066i001p00259

Karato, S. (2008). *Deformation of Earth Materials.* New York: Cambridge University Press. https://doi.org/10.1017/CBO9780511804892

Karato, S. (2010). Rheology of the Earth's mantle: A historical review. *Gondwana Research, 18*(1), 17-45. https://doi.org/10.1016/j.gr.2010.03.004

Karato, S., & Jung, H. (2003). Effects of pressure on high-temperature dislocation creep in olivine. *Philosophical magazine, 83*(3), 401-414. https://doi.org/10.1080/0141861021000025829

Kelemen, P. B., & Manning, C. E. (2015). Reevaluating carbon fluxes in subduction zones, what goes down, mostly comes up. *Proceedings of the National Academy of Sciences, 112*(30), E3997-E4006. https://doi.org/10.1073/pnas.1507889112

Kerrick, D. M., & Connolly, J. A. D. (2001). Metamorphic devolatilization of subducted marine sediments and the transport of volatiles into the Earth's mantle. *Nature*, 411, 293-296. https://doi.org/10.1038/35077056

Kerschhofer, L., Dupas, C., Liu, M., Sharp, T. G., Durham, W. B., & Rubie, D. C. (1998). Polymorphic transformations between olivine, wadsleyite and ringwoodite: Mechanisms of intracrystalline nucleation and the role of elastic strain. *Mineralogical Magazine, 62*(5), 617-638. https://doi.org/10.1180/002646198548016

Kirby, S. H., Durham, W. B., & Stern, L. A. (1991). Mantle phase changes and deep-earthquake faulting in subducting lithosphere. *Science, 252*(5003), 216-225. https://doi.org/10.1126/science.252.5003.216

Kirby, S. H., Stein, S., Okal, E. A., & Rubie, D. C. (1996). Metastable mantle phase transformations and deep earthquakes in subducting oceanic lithosphere. *Reviews of Geophysics, 34*(2), 261-306. https://doi.org/10.1029/96RG01050

Kohlstedt, D. L., Evans, B., & Mackwell, S. J. (1995). Strength of the lithosphere: Constraints imposed by laboratory experiments. *Journal of Geophysical Research: Solid Earth, 100*(B9), 17587-17602. https://doi.org/10.1029/95JB01460

Kristiansen, K., Valtiner, M., Greene, G. W., Boles, J. R., & Israelachvili, J. N. (2011). Pressure solution – the importance of the electrochemical surface potentials. *Geochimica et Cosmochimica Acta, 75*(22), 6882-6892. https://doi.org/10.1016/j.gca.2011.09.019

Larché, F., & Cahn, J. W. (1973). A linear theory of thermochemical equilibrium of solids under stress. *Acta Metallurgica, 21*(8), 1051-1063. https://doi.org/10.1016/0001-6160(73)90021-7

Larché, F., & Cahn, J. W. (1978a). A nonlinear theory of thermochemical equilibrium of solids under stress. *Acta Metallurgica, 26*(1), 53-60. https://doi.org/10.1016/0001-6160(78)90201-8

Larché, F., & Cahn, J. W. (1978b). Thermochemical equilibrium of multiphase solids under stress. *Acta Metallurgica, 26*(10), 1579-1589. https://doi.org/10.1016/0001-6160(78)90067-6

Larché, F., & Cahn, J. W. (1985). Overview no. 41 The interactions of composition and stress in crystalline solids. *Acta Metallurgica, 33*(3), 331-357. https://doi.org/10.1016/0001-6160(85)90077-X

Little, T. A., Baldwin, S. L., Fitzgerald, P. G., & Monteleone, B. (2007). Continental rifting and metamorphic core complex formation ahead of the Woodlark spreading ridge, D'Entrecasteaux Islands, Papua New Guinea. *Tectonics, 26*(1), TC1002. https://doi.org/10.1029/2005TC001911

915 Llana-Fúnez, S., Wheeler, J., & Faulkner, D. R. (2012). Metamorphic reaction rate controlled by
916 fluid pressure not confining pressure: implications of dehydration experiments with
917 gypsum. *Contributions to Mineralogy and Petrology, 164*(1), 69-79.
918 https://doi.org/10.1007/s00410-012-0726-8
919 McNamara, A. K., van Keken, P. E., Karato, S. (2002). Development of anisotropic structure in
920 the Earth's lower mantle by solid-state convection. *Nature*, 416, 310-314.
921 https://doi.org/10.1038/416310a
922 Mikowski, A., Soares, P., Wypych, F., & Lepienski, C. M. (2008). Fracture toughness, hardness,
923 and elastic modulus of kyanite investigated by a depth-sensing indentation technique.
924 *American Mineralogist, 93*(5-6), 844-854. https://doi.org/10.2138/am.2008.2694
925 Moore, J., Beinlich, A., Austrheim, H., & Putnis, A. (2019). Stress orientation-dependent
926 reactions during metamorphism. *Geology, 47*(2), 151-154.
927 https://doi.org/10.1130/G45632.1
928 Mosenfelder, J. L., Marton, F. C., Ross, C. R., Kerschhofer, L., & Rubie, D. C. (2001).
929 Experimental constraints on the depth of olivine metastability in subducting lithosphere.
930 *Physics of the Earth and Planetary Interiors, 127*(1-4), 165-180.
931 https://doi.org/10.1016/S0031-9201(01)00226-6
932 Moulas, E., Schmalholz, S. M., Podladchikov, Y., Tajčmanová, L., Kostopoulos, D., &
933 Baumgartner, L. (2019). Relation between mean stress, thermodynamic, and lithostatic
934 pressure. *Journal of Metamorphic Geology*, *37*(1), 1-14.
935 https://doi.org/10.1111/jmg.12446
936 Nye, J. F. (1957). *Physical properties of crystals*. New York: Oxford University Press.

Pabst, W., & Gregorova, E. (2013). Elastic properties of silica polymorphs – a review. *Ceramics-Silikáty, 57*(3), 167-184.

Paterson, M. S. (1973). Nonhydrostatic thermodynamics and its geological applications. *Reviews of Geophysics and Space Physics, 11*(2), 355-389.

Peterman, E. M., Hacker, B. R., & Baxter, E. F. (2009). Phase transformations of continental crust during subduction and exhumation: Western Gneiss Region, Norway. *European Journal of Mineralogy, 21*(6), 1097-1118. https://doi.org/10.1127/0935-1221/2009/0021-1988

Plümper, O., John, T., Podladchikov, Y. Y., Vrijmoed, J. C., & Scambelluri, M. (2017). Fluid escape from subduction zones controlled by channel-forming reactive porosity. *Nature Geoscience*, 10, 150-156. https://doi.org/10.1038/ngeo2865

Powell, R., Evans, K. A., Green, E. C. R., & White, R. W. (2018). On equilibrium in non-hydrostatic metamorphic systems. *Journal of Metamorphic Geology, 36*(4), 419-438. https://doi.org/10.1111/jmg.12298

Putnis, A., & Austrheim, H. (2010). Fluid-induced processes: metasomatism and metamorphism. *Geofluids, 10*(1-2), 254-269. https://doi.org/10.1111/j.1468-8123.2010.00285.x

Putnis, A., & John, T. (2010). Replacement processes in the Earth's crust. *Elements, 6*(3), 159-164. https://doi.org/10.2113/gselements.6.3.159

Richter, B., Stünitz, H., & Heilbronner, R. (2016). Stresses and pressures at the quartz-to-coesite phase transformation in shear deformation experiments. *Journal of Geophysical Research: Solid Earth, 121*(11), 8015-8033. https://doi.org/10.1002/2016JB013084

Robin, P. F. (1978). Pressure solution at grain-to-grain contacts. *Geochimica et Cosmochimica Acta, 42*(9), 1383-1389. https://doi.org/10.1016/0016-7037(78)90043-1

960 Rubie, D. C., & Ross, C. R. (1994). Kinetics of the olivine-spinel transformation in subducting
961 lithosphere: experimental constraints and implications for deep slab processes. *Physics of*
962 *the Earth and Planetary Interiors, 86*(1-3), 223-243. https://doi.org/10.1016/0031-
963 9201(94)05070-8
964 Rutter, E. H. (1983). Pressure solution in nature, theory and experiment. *Journal of Geological*
965 *Society, 140*(5), 725-740. https://doi.org/10.1144/gsjgs.140.5.0725
966 Rybacki, E., Konrad, K., Renner, J., Wachmann, M., Stöckhert, B., & Rummel, F. (2003).
967 Experimental deformation of synthetic aragonite marble. *Journal of Geophysical*
968 *Research: Solid Earth*, *108*(B3), 2174. https://doi.org/10.1029/2001JB000694
969 Schön, S. J. (2011). Elastic Properties. In *Physical Properties of Rocks* (Vol. 8, pp. 149–243).
970 Great Britain: Elsevier. https://doi.org/10.1016/S1567-8032(11)08006-2
971 Schubnel, A., Brunet, F., Hilairet, N., Gasc, J., Wang, Y., & Green, H. W. (2013). Deep-focus
972 earthquakes analogs recorded at high pressure and temperature in the laboratory. *Science,*
973 *341*(6152), 1377-1380. https://doi.org/10.1126/science.1240206
974 Sekerka, R. F., & Cahn, J. W. (2004). Solid-liquid equilibrium for non-hydrostatic stress. *Acta*
975 *Materialia, 52*(6), 1663-1668. https://doi.org/10.1016/j.actamat.2003.12.010
976 Shi, S., Markmann, J., & Weissmüller, J. (2018). Verifying Larché-Cahn elasticity, a milestone
977 of 20th-century thermodynamics. *Proceedings of the National Academy of Sciences,*
978 *115*(43), 10914-10919. https://doi.org/10.1073/pnas.1809355115
979 Stewart, E. M., & Ague, J. J. (2020). Pervasive subduction zone devolatilization recycles CO2
980 into the forearc. *Nature Communications*, 11, 6220. https://doi.org/10.1038/s41467-020-
981 19993-2

Tajčmanová, L., Podladchikov, Y., Powell, R., Moulas, E., Vrijmoed, J. C., & Connolly, J. A. D. (2014). Grain-scale pressure variations and chemical equilibrium in high-grade metamorphic rocks. *Journal of Metamorphic Geology, 32*(2), 195-207. https://doi.org/10.1111/jmg.12066

Tajčmanová, L., Vrijmoed, J., & Moulas, E. (2015). Grain-scale pressure variations in metamorphic rocks: implications for the interpretation of petrographic observations. *Lithos*, 216-217, 338-351. https://doi.org/10.1016/j.lithos.2015.01.006

Vaughan, P. J., Green, H. W., & Coe, R. S. (1984). Anisotropic growth in the olivine-spinel transformation of Mg2GeO4 under nonhydrostatic stress. *Tectonophysics, 108*(3-4), 299-322. https://doi.org/10.1016/0040-1951(84)90241-5

Voorhees, P. W., & Johnson, W. C. (2004). The thermodynamics of elastically stressed crystals. *Solid State Physics*, 59, 1-201. https://doi.org/10.1016/S0081-1947(04)80003-1

Wenk, H. (1985). *Preferred orientation in deformed metals and rocks: an introduction to modern texture analysis*. Orlando: Academic Press.

Wheeler, J. (2014). Dramatic effects of stress on metamorphic reactions. *Geology, 42*(8), 647-650. https://doi.org/10.1130/G35718.1

Wheeler, J. (2018). The effects of stress on reactions in the Earth: Sometimes rather mean, usually normal, always important. *Journal of Metamorphic Geology, 36*(4), 439-461. https://doi.org/10.1111/jmg.12299

Wheeler, J. (2020). A unifying basis for the interplay of stress and chemical processes in the Earth: support from diverse experiments. *Contributions to Mineralogy and Petrology*, 175, 116. https://doi.org/10.1007/s00410-020-01750-9

1004 Yoshino, T., Mibe, K., Yasuda, A., & Fujii, T. (2002). Wetting properties of anorthite
1005 aggregates: Implications for fluid connectivity in continental lower crust. *Journal of*
1006 *Geophysical Research: Solid Earth, 107*(B1), ECV-10.
1007 https://doi.org/10.1029/2001JB000440
1008 Zhou, Y., He, C., Song, J., Ma, S., & Ma, J. (2005). An experiment study of quartz-coesite
1009 transition at differential stress. *Chinese Science Bulletin, 50*(5), 446-451.
1010 https://doi.org/10.1007/BF02897461
1011 Zulauf, G. (2001). Structural style, deformation mechanisms and paleodifferential stress along an
1012 exposed crustal section: constraints on the rheology of quartzofeldspathic rocks at supra-
1013 and infrastructural levels (Bohemian Massif). *Tectonophysics, 332*(1-2), 211-237.
1014 https://doi.org/10.1016/S0040-1951(00)00258-4